GEOPHYSICS, VOL. 73, NO. 2 (MARCH-APRIL 2008); P. C7–C12, 7 FIGS., 3 TABLES.
10.1190/1.2837641

Experimental verification of spherical-wave effect on the AVO response and implications for three-term inversion

Mohammed Alhussain[1], Boris Gurevich[2], and Milovan Urosevic[3]

ABSTRACT

Spherical-wave offset-dependent reflectivity is investigated by measuring ultrasonic reflection amplitudes from a water/Plexiglas interface. The experimental results show substantial deviation of the measured amplitudes from the plane-wave reflection coefficients at large angles. However, full-wave numerical simulations of the point source reflection response using the reflectivity algorithm show excellent agreement with the measurements, demonstrating that the deviation from the plane-wave response is caused by the wavefront curvature. To analyze the effect of wavefront curvature on elastic inversion, we simulate the spherical-wave reflectivity at different frequencies and invert for elastic parameters by least-square fitting of the plane-wave (Zoeppritz) solution. The results show that the two-parameter inversion based on the intercept and gradient is robust, although estimation of three parameters (V_P, V_S, and density) that use the curvature of the offset variation with angle (AVA) response is prone to substantial frequency-dependent errors. We propose an alternative approach to parameter estimation, one that uses critical angles estimated from AVA curves (instead of the AVA curvature). This approach shows a significant improvement in the estimation of elastic parameters, and it could be applied to class 1 AVO responses.

INTRODUCTION

Most amplitude variation with offset (AVO) analysis and inversion techniques employed today are based on the Zoeppritz equations for plane-wave reflection coefficients or their linearized approximations (Downton and Ursenbach, 2006). At the same time, seismic surveys use localized sources that produce spherical rather than plane waves, and it is well known that the AVO response for spherical waves differs from plane waves (Červený, 1961; Krail and Brysk, 1983). Winterstein and Hanten (1985) show that AVO amplitudes of nonplanar (cylindrical) waves are much closer to real data than those provided by plane-wave modeling. This effect is particularly large for angles approaching the critical angle, where amplitude values are considerably smaller than those predicted by plane-wave theory. Recent work by Haase (2004) and Haase and Ursenbach (2007) highlight the importance of spherical-wave AVO effects for rock property estimation.

The plane-wave approximation for reflection coefficients is justified for exploration target horizons in the far-field (usually at depths of 10–20 wavelengths) where wavefront curvature is small. This approximation is adequate for moderate angles of incidence, well below the critical angle. Because the conventional (two-term) AVO analysis assumes moderate offsets and angles, the use of the plane-wave Zoeppritz equations is justified.

Conventional linear AVO analysis allows the extraction of two parameters, such as P- and S-wave impedance contrasts, and requires additional a priori information about the velocity-density relationship and/or Poisson's ratio. The introduction of longer spreads and improved processing methods in recent years has enabled recording and preservation of long-offset amplitudes. In principle, the use of these long offsets permits the extraction of three independent parameters such as relative contrasts in compressional and shear velocities, V_P and V_S, and density ρ (Kelly et al., 2001). However, as shown by Haase (2004) and van der Baan and Smit (2006), the plane-wave approximation becomes increasingly inaccurate for large incidence angles close to the critical angle, which makes the three-parameter inversion inadequate.

We verify the spherical wave effect on the AVO response by performing laboratory ultrasonic measurements of the P-P reflection response for a water/Plexiglas interface. To analyze the nature of the observed response, we first compare it with the plane-wave reflection coefficients computed with Zoeppritz equations. This compari-

Manuscript received by the Editor 24 July 2007; revised manuscript received 1 November 2007; published online 27 February 2008.
[1]Formerly Curtin University of Technology, Department of Exploration Geophysics; presently Saudi Aramco, Dhahran, Saudi Arabia. E-mail: mohammed.hussain.3@aramco.com.
[2]Curtin University of Technology, Department of Exploration Geophysics, Perth, Australia, and CSIRO Petroleum, Bentley, Australia. E-mail: B.Gurevich@curtin.edu.au.
[3]Curtin University of Technology, Department of Exploration Geophysics, Perth, Australia. E-mail: M.Urosevic@curtin.edu.au.

son shows substantial differences between the measured and predicted response at large angles close to the critical angle. To understand this effect, we then perform full-wave numerical simulations with a point source, which agrees with the measurements at all offsets. This agreement highlights the role of the wavefront curvature in reflection phenomena and suggests that the failure to account for it may lead to errors in elastic inversion.

Because standard AVO analysis usually considers the reflection response at small and moderate angles, the effect of wavefront curvature is unlikely to cause large errors. However, this effect can cause significant distortions in three-term AVO parameter estimation (usually aimed at estimation of the velocities and density) because such estimation requires large-offset amplitude. To analyze these errors, we perform full-wave numerical simulations of the spherical-wave reflection response at a range of frequencies. Each of these responses is then inverted for three parameters (V_P, V_S, and density) using a least-square fitting routine based on the full Zoeppritz equations. As expected, the plane-wave inversion of a spherical wave response yields significant errors in the estimates of elastic parameters. We then propose an alternative approach to three-parameter inversion, which involves estimation of the critical angle from the amplitude variation with angle (AVA) curve. Application of this new algorithm to both experimental and synthetic data shows promising results.

Table 1. The elastic parameters of the Plexiglas model and water. Velocities are in kilometers per second and densities in grams per cubic centimeter.

Plexiglas			Water	
V_P	V_S	ρ	V_{P0}	ρ_0
2.724	1.384	1.2	1.484	1

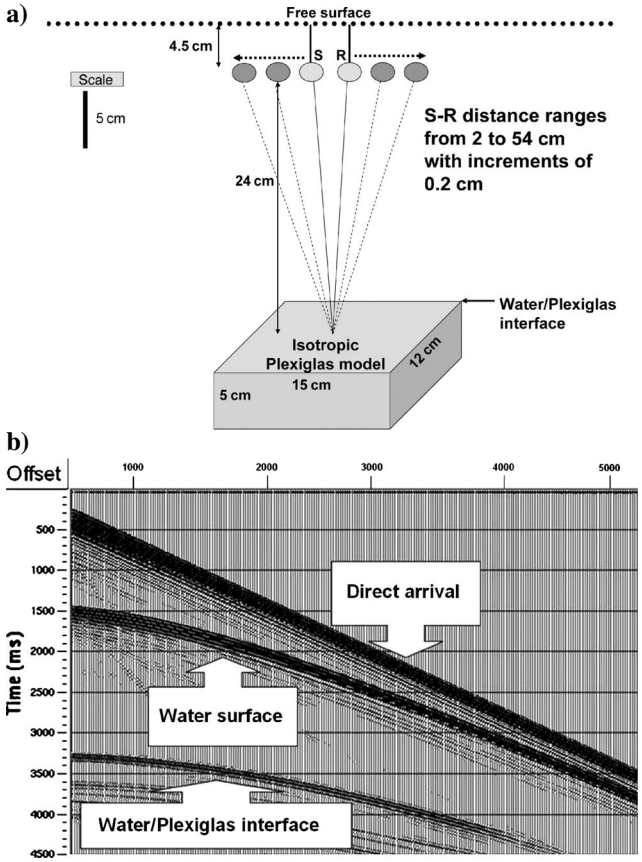

Figure 1. (a) Acquisition parameters of the reflection measurement for water/Plexiglas interface producing CMP gather (b) with three seismic events indicated by arrows.

EXPERIMENT

Seismic wave propagation and partitioning of energy at an interface can be effectively studied using physical modeling, whereby models are constructed so that they resemble real geologic structures taking into account the distance scale factor. Hence, by using scaled models in a controlled environment, it can be assumed that the response from the models is the same as the response from real earth materials. An advantage of laboratory experiments is that real seismic waves propagate through models with no numerical approximations.

Laboratory AVO experiments were conducted using equipment at the Curtin University physical modeling laboratory (Luo and Evans, 2004). The system comprises a set of computer-controlled ultrasonic piezoelectric transducers operating as seismic sources and receivers. Movement of transducers is controlled in three dimensions by high-precision stepping motors. A data acquisition program written using LabVIEW, a National Instruments proprietary programming system for signal control, acquisition, and analysis (Mihura, 2001), enables versatile source-receiver configurations including transmission measurements 2D, 3D, and VSP surveys.

Physical properties of model materials need to be precisely measured. For solid media, these include P- and S-wave velocities and densities. Plexiglas is often a material of choice because it is intrinsically isotropic and has a P-wave velocity of about 2700 m/s, which provides a good velocity contrast with a water column. Plexiglas has a density of 1.2 g/cm^3, which allows the material to be submerged in a water tank.

To obtain properties of Plexiglas (required as input parameters for numerical simulations), we performed a set of transmission measurements. The sound velocity in water was measured also to ensure accurate numerical simulations. Resulting properties for both Plexiglas model and water are shown in Table 1.

We then performed a reflection experiment to analyze angle-dependent reflectivity of the water/Plexiglas interface, where the Plexiglas model was submerged in a water tank. Omni-directional cylindrical P-wave transducers with a 220-kHz-dominant frequency were submerged in water also and positioned 24 cm above the model. Common midpoint (CMP) recording was employed for data acquisition. The minimum offset was 2 cm, and source and receivers were moved apart at increments of 1 mm in opposite directions. A total of 270 CMP traces were recorded over the model. At each position, 20 CMP traces were acquired and vertically stacked to increase the signal-to-noise ratio (S/N). With a scaling factor of 1:10,000, this model simulated 20-m-trace spacing and a source wavelet of 22 Hz dominant frequency reflecting from an interface at a depth of 2.4 km. The acquisition parameters and the resulting CMP gather are shown in Figure 1a and b.

NUMERICAL SIMULATIONS AND COMPARISON

To obtain water/Plexiglas reflection coefficients R_{PP} from the gathers (Figure 1b), we picked the amplitudes of the water/Plexiglas

reflection, corrected them for geometrical spreading, and calibrated them at the near offset to the theoretical zero-offset reflection coefficient. The resulting R_{PP} values are plotted in Figure 2 as a function of incidence angle θ. Also shown in Figure 2 are theoretical plane-wave (Zoeppritz) reflection coefficients computed from elastic parameters extracted from transmission measurements. The plane-wave solution agrees very well with the physical modeling data for moderate angles of incidence (up to 20°–25°). On the other hand, a big discrepancy occurs at large angles, especially those close to the critical angle. This is a known effect caused by wavefront curvature (Krail and Brysk, 1983; Haase, 2004; Doruelo et al., 2006; van der Baan and Smit, 2006; Ursenbach et al., 2007).

Physically, this effect can be explained by the fact that the spherical wave (or indeed any wave with a curved wavefront) can be considered as an infinite sum (integral) of plane waves with different angles to the vertical. At any given point of the interface, the reflection of the spherical wave involves reflection not of just one plane wave corresponding to the specular ray but a range of plane waves corresponding to the bunch of rays within the ray beam around the central ray. Thus, the amplitude of the reflected wave can be thought of as an average of plane-wave reflection coefficient over a range of incident angles around the ray angle. When the variation of the plane-wave reflection coefficient with incidence angle is gradual (as at angles below 20°–25°), the averaging has very little effect.

However, when the reflection coefficient changes rapidly, as it does in the vicinity of the critical angle, the averaging smoothes over the reflection coefficient and causes the deviation of the reflection amplitude from the plane-wave reflection coefficient. The magnitude of this effect depends on the averaging aperture, which is controlled by the size of the Fresnel zone (and thus depends on both the frequency and the distance between the source and the interface). In addition, at postcritical angles the curved wavefront generates a head wave, which forms a complex interference pattern with the postcritical reflection.

To account for spherical wave effects, we performed numerical simulations with a full-wave algorithm based on a numerical solution of the full elastic wave equations with a point source. We simulated the AVA response using a recursive frequency-wavenumber domain reflectivity algorithm (Aki and Richards, 1980; Kennett, 1980, 1983). The resulting amplitudes picked on seismograms and corrected for geometric spreading are also shown in Figure 2. We can see an excellent agreement between laboratory-measured AVO response for the water/Plexiglas interface and numerical simulations. This result indicates that the laboratory measurements are accurate and the spherical approximation of the radiation pattern of the transducers is appropriate. The excellent match confirms the effect of a spherical wave on the AVO response and how spherical wave AVO responses differ from plane-wave AVO responses.

To analyze the effect of this difference on the AVO attributes, in Figure 3 we replotted both experimental and theoretical reflection coefficients (for plane and spherical waves) against $\sin^2\theta$. Spherical and plane-wave AVO responses have almost the same normal incidence (intercept) and slope (gradient) but very different curvature terms. The agreement for small offsets is understandable because the reflector is well within the far-field (depth-to-wavelength ratio is about 36). However, somewhat surprisingly, we find that the far-field (or high-frequency) approximation is nevertheless invalid at larger angles. To understand this effect, we simulated the point source AVA response at different frequencies.

The results for frequencies 50, 100, 220, and 400 kHz are plotted against $\sin^2\theta$ in Figure 4. The curves show no difference in intercept and gradient terms, but the curvature at larger angles (over 25°) is frequency dependent. Thus, we expect that the frequency dependence of reflection coefficients will not affect conventional two-term AVO analysis, but it can distort the results of a three-parameter inversion if the latter is performed using plane-wave Zoeppritz solution or its linear approximations.

THREE-TERM AVO INVERSION

To analyze the effect of frequency on parameter extraction from reflection coefficients, we implemented a least-squares inversion routine to find the medium parameters that give the best match between a given AVA curve (experimental or simulated) and the Zoeppritz plane-wave solution. In this single-interface inversion, we

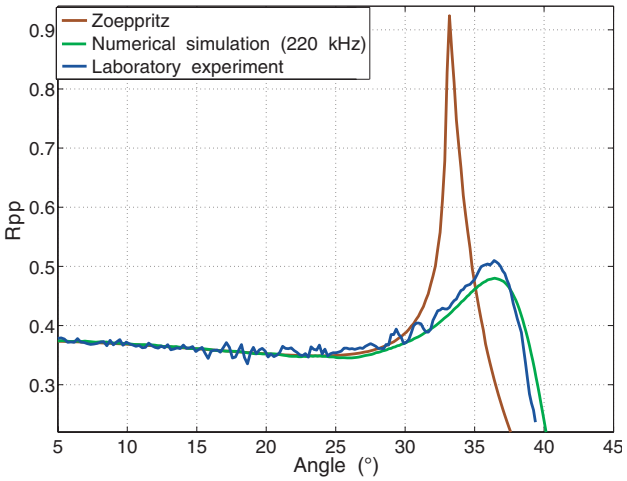

Figure 2. Comparison of measured reflection coefficients versus incidence angle for water/Plexiglas interface (blue line) with plane-wave response computed with Zoeppritz equations (brown line) and point-source numerical simulation (green line).

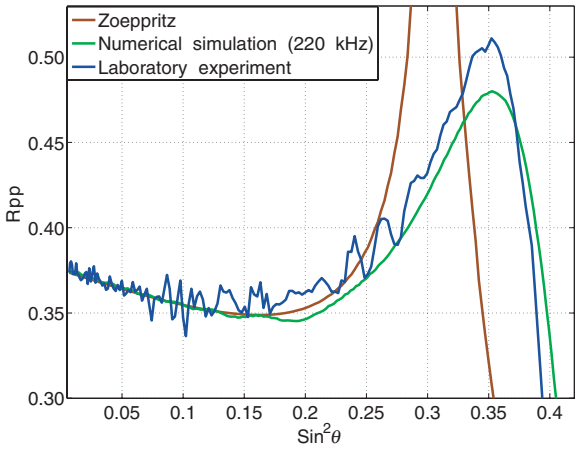

Figure 3. Comparison of measured reflection coefficients versus $\sin^2\theta$ for water/Plexiglas interface (blue line) with plane-wave response computed with Zoeppritz equations (brown line) and point-source numerical simulation (green line).

searched for three parameters of the lower medium: P- and S-wave velocities V_P and V_S and density ρ, assuming that the properties of the upper medium V_{P0}, V_{S0}, and ρ_0 are known.

The spherical wave reflection responses at different frequencies, along with the best plane-wave approximations, are shown in Figure 5. The extracted parameters (V_P, V_S, and ρ, as well as P- and S-impedances Z_P and Z_S) are listed in Table 2. It can be seen from Figure 6 that as the frequency decreases, the extracted impedances show little variation ($<1\%$ for Z_P and $<4\%$ for Z_S) whereas V_P, V_S, and density show strong variation (up to 20%).

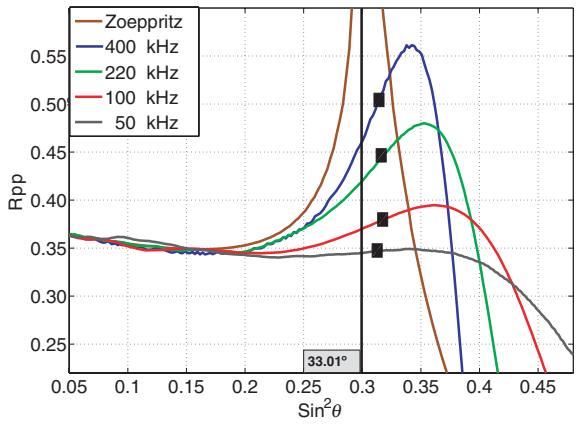

Figure 4. Simulated AVA responses at different frequencies plotted against $\sin^2\theta$. Squares denote inflection points used to estimate critical angles. Brown line is the plane-wave response computed with the Zoeppritz equations.

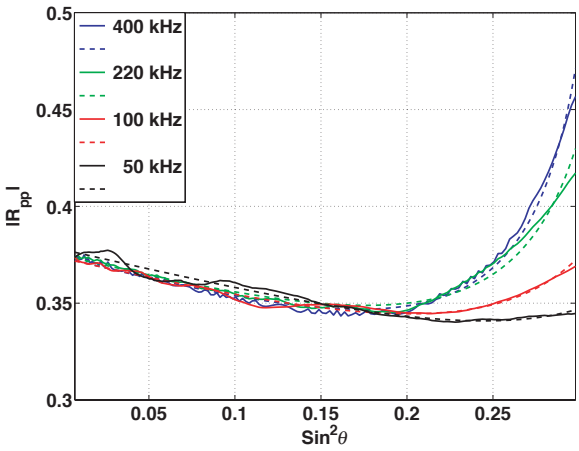

Figure 5. The spherical wave AVA responses at different frequencies along with the best-fit plane-wave approximations.

Table 2. The resulting extracted parameters using three-term AVO inversion. Velocities are in kilometers per second and densities in grams per cubic centimeter.

Parameters	V_P	V_S	ρ	Z_P	Z_S
True values	2.724	1.384	1.2	3.269	1.661
400 kHz	2.635	1.327	1.237	3.259	1.642
220 kHz	2.580	1.280	1.266	3.267	1.621
100 kHz	2.435	1.188	1.337	3.256	1.589
50 kHz	2.294	1.123	1.434	3.290	1.611
Laboratory	2.549	1.187	1.278	3.257	1.516

INVERSION USING CRITICAL ANGLES

The fact that extraction of impedances is more robust than simultaneous extraction of velocities and densities is well known, because at moderate offsets the reflection coefficients are mainly sensitive to P- and S-impedance contrasts. To extract all three parameters, we must use large offsets where reflection amplitudes differ from the plane-wave response. One way to overcome this difficulty is to use information about the critical angle. The critical angle corresponds to the singularity of the plane-wave reflection coefficient, and our first idea was to pick the maximum of the AVA curve. However, as we see in Figure 4, the position of the peak of Rpp also varies with frequency. Landro and Tsvankin (2007) suggest that the position of the inflection point (the point of the fastest increase) of the AVA curve is more stable and is a good proxy for the critical angle.

To reduce the parameter extraction errors caused by spherical wave effects, we propose incorporating critical angles as measured by the position of the inflection point on AVA curves. The proposed workflow is as follows:

1) The critical angle θ_{cr} is picked from the AVA curve as the angle corresponding to the inflection point.
2) The P-wave velocity of the lower medium is computed using Snell's law: $V_P = V_{P0}/\sin\theta_{cr}$.
3) Plane-wave inversion routine is used to extract P- and S-impedances only (using angles up to 20°).
4) Density is calculated as $\rho = Z_P/V_P$.
5) S-wave velocity V_S is computed from Z_S and density: $V_S = Z_S/\rho$.

We applied the above methodology to both numerically simulated and experimental AVA curves shown in Figures 3 and 4. The inflection points are shown on AVA curves in Figure 4. The extracted parameters are presented in Table 3. We see that the critical angle-based inversion method gives much better estimates of all three parameters than the curvature-based method (Figure 7). The errors in any parameters do not exceed 5%, except for the lowest frequency of 50 kHz.

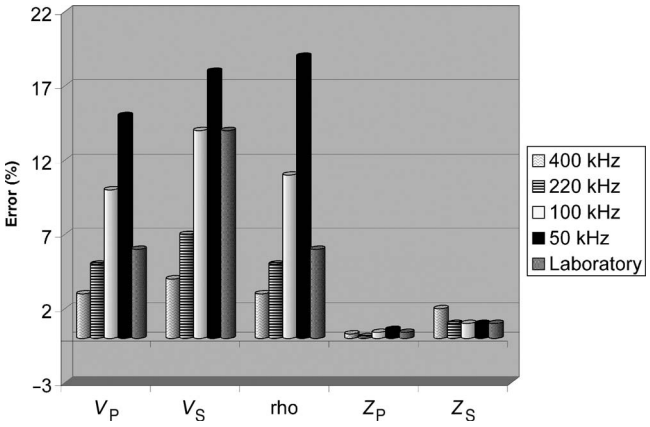

Figure 6. Departure of extracted parameters using three-term AVO inversion from true values shown in error percentages.

Table 3. The new extracted parameters using the new inversion method. Velocities are in kilometers per second and densities in grams per cubic centimeter.

Parameters	V_P	V_S	ρ	Z_P	Z_S
True values	2.724	1.384	1.2	3.269	1.661
400 kHz	2.689	1.399	1.217	3.272	1.702
220 kHz	2.691	1.392	1.219	3.280	1.697
100 kHz	2.694	1.308	1.211	3.262	1.583
50 kHz	2.707	1.471	1.223	3.309	1.799
Laboratory	2.704	1.380	1.217	3.292	1.680

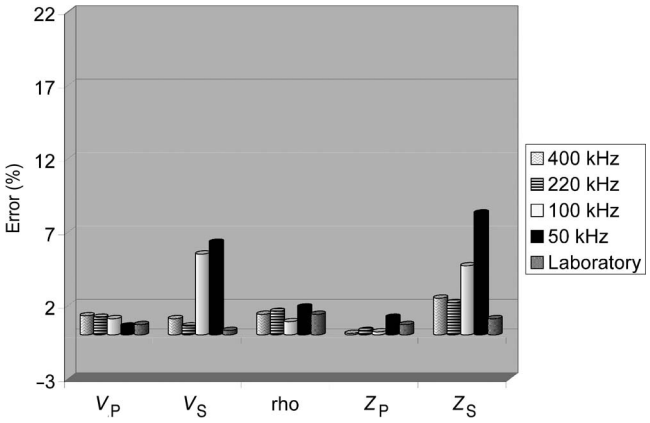

Figure 7. Departure of extracted parameters using the new inversion method (using critical angles) from true values shown in error percentages.

An obvious limitation of the proposed technique is the requirement of a large and positive contrast between the velocities of the upper and lower media ($V_P > V_{P0}$), which corresponds to class 1 AVO. Of course, we need long offsets and good signal-to-noise ratios. Careful and special processing steps are needed to preserve the true long offset reflected amplitudes. In the case of low frequency, critical angles are hard to pick because the fastest amplitude increase is not evident even for noise-free numerical simulations. (See our example for 50 kHz frequency, Figure 4). Above all, this procedure is only applicable to an isolated reflection from a single interface.

Van der Baan and Smith (2006) propose a different methodology of AVO inversion that is based on the transformation of common-shot gathers to plane-wave gathers using the tau-p transform. This is a promising approach for multilayered elastic inversion.

CONCLUSIONS

To investigate spherical wave reflectivity in the laboratory, we performed ultrasonic measurements of the P-P reflection response for a water/Plexiglas interface. The measured P-P reflection response agrees very well with the plane-wave response (as computed using Zoeppritz equations) at small-to-moderate incidence angles (up to 20°–25°), but it shows substantial deviation from the plane-wave reflection coefficients at large angles. To analyze this deviation, we have generated full-wave point source reflectivity simulations. These simulations show excellent agreement with the laboratory experiment, demonstrating that the deviation of the reflection response from the plane-wave (Zoeppritz) solution is caused by the effect of the wavefront curvature. Although theoretically these effects are well known, our results appear to provide the first experimental validation of the theoretical and numerical predictions of the long-offset behavior of the reflection response in controlled laboratory conditions.

Because AVO/AVA analysis and inversion usually utilize reflection response at small and moderate angles, the effect of the wavefront curvature is unlikely to cause significant errors. However, this effect can cause significant distortions in three-term AVA parameter estimation (often used to estimate separately the velocities and density), because this estimation requires large offset information. To analyze these distortions, we computed full-wave numerical simulations of the spherical wave reflection response for a range of frequencies. Each of these responses was then inverted for three parameters (V_P, V_S, and density) using a least-square fitting routine based on the full Zoeppritz equations. The resulting estimates of P- and S-impedances are robust, but estimates of V_P, V_S, and density show substantial frequency-dependent errors caused by wavefront curvature effect.

We then proposed an alternative approach for three-parameter inversion, one that involves estimation of the critical angle from the AVA curve. This approach shows a significant improvement in parameter estimation. Although the assumptions behind the proposed algorithm make it too restrictive to be practical, the approach highlights the need for further developments in long offset AVO inversion.

ACKNOWLEDGMENTS

We are grateful to Brian Evans, Bruce Hartley, and Mark Lwin for help with laboratory experiments. We also thank Enru Liu, Abdullah Al-Ramadhan, Marcos Grochau, and Putri Wisman for useful discussions. Alhussain thanks Saudi Aramco for his Master's Degree scholarship. The financial support of the sponsors of the Curtin Reservoir Geophysics Consortium is gratefully acknowledged.

REFERENCES

Aki, K., and P. G. Richards, 1980, Quantitative seismology: University Science Books.

Červený, V., 1961, The amplitude curves of reflected harmonic waves around the critical point: Studia Geophysica et Geodaetica, **5**, 319–351.

Doruelo, J., F. Hilterman, and G. Goloshubin, 2006, Head waves as mechanism for azimuthal PP AVO magnitude anomalies: 76th Annual International Meeting, SEG, Expanded Abstracts, 199–203.

Downton, J. E., and C. Ursenbach, 2006, Linearized amplitude variation with offset (AVO) inversion with supercritical angles: Geophysics, **71**, no. 5, E49–E55.

Haase, A. B., 2004, Spherical wave AVO modeling of converted waves in isotropic media: 74th Annual International Meeting, SEG, Expanded Abstracts, 263–266.

Haase, A. B., and C. P. Ursenbach, 2007, Spherical-wave computational AVO modelling in elastic and anelastic isotropic two-layer media: 69th Annual Conference and Exhibition, EAGE, Extended Abstracts.

Kelly, M., C. Skidmore, and D. Ford, 2001, AVO inversion, Part 1: Isolating rock property contrasts: The Leading Edge, **20**, 230–323.

Kennett, B. L. N., 1980, Seismic waves in a stratified half space — II. Theoretical seismograms: Geophysical Journal of the Royal Astronomical Society, **61**, 1–10.

———, 1983, Seismic wave propagation in stratified media: Cambridge University Press.

Krail, P. M., and H. Brysk, 1983, Reflection of spherical seismic waves in elastic layered media: Geophysics, **48**, 655–664.

Landro, M., and I. Tsvankin, 2007, Seismic critical-angle reflectometry?: A method to characterize azimuthal anisotropy?: Geophysics, **72**, no. 3, D41–D50.
Luo, M., and B. J. Evans, 2004, An amplitude-based multiazimuth approach to mapping fractures using P-wave 3D seismic data: Geophysics, **69**, 690–698.
Mihura, B., 2001, LabVIEW for data acquisition: Prentice-Hall, Inc.
Ursenbach, C. P., A. B. Haase, and J. E. Downton, 2007, Improved modelling for spherical-wave AVO: 69th Annual Conference and Exhibition, EAGE, Extended Abstracts.
van der Baan, M., and D. Smit, 2006, Amplitude analysis of isotropic P-wave reflections: Geophysics, **71**, no. 6, C93–C103.
Winterstein, D. F., and J. B. Hanten, 1985, Supercritical reflections observed in P- and S-wave data: Geophysics, **50**, 185–195.